JOURNAL OF Applied Polymer SCIENCE

Special Issue: Microfiltration and Ultrafiltration Membrane Science and Technology

Guest Editors: Prof. Isabel C. Escobar (University of Toledo) and Prof. Bart Van der Bruggen (University of Leuven)

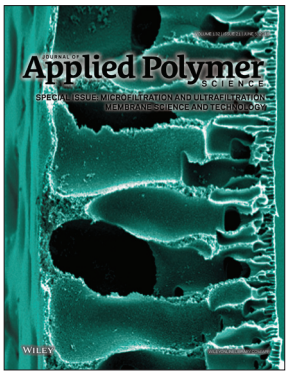

EDITORIAL

Microfiltration and Ultrafiltration Membrane Science and Technology
I. C. Escobar and B. Van der Bruggen, *J. Appl. Polym. Sci.* 2015, **DOI: 10.1002/app.42002**

REVIEWS

Nanoporous membranes generated from self-assembled block polymer precursors: *Quo Vadis*?
Y. Zhang, J. L. Sargent, B. W. Boudouris and W. A. Phillip, *J. Appl. Polym. Sci.* 2015, **DOI: 10.1002/app.41683**

Making polymeric membranes anti-fouling via "grafting from" polymerization of zwitterions
Q. Li, J. Imbrogno, G. Belfort and X.-L. Wang, *J. Appl. Polym. Sci.* 2015, **DOI: 10.1002/app.41781**

Fouling control on MF/ UF membranes: Effect of morphology, hydrophilicity and charge
R. Kumar and A. F. Ismail, *J. Appl. Polym. Sci.* 2015, **DOI: 10.1002/app.42042**

EMERGING MATERIALS AND FABRICATION

Preparation of a poly(phthalazine ether sulfone ketone) membrane with propanedioic acid as an additive and the prediction of its structure
P. Qin, A. Liu and C. Chen, *J. Appl. Polym. Sci.* 2015, **DOI: 10.1002/app.41621**

Preparation and characterization of MOF-PES ultrafiltration membranes
L. Zhai, G. Li, Y. Xu, M. Xiao, S. Wang and Y. Meng, *J. Appl. Polym. Sci.* 2015, **DOI: 10.1002/app.41663**

Tailoring of structures and permeation properties of asymmetric nanocomposite cellulose acetate/silver membranes
A. S. Figueiredo, M. G. Sánchez-Loredo, A. Maurício, M. F. C. Pereira, M. Minhalma and M. N. de Pinho, *J. Appl. Polym. Sci.* 2015, **DOI: 10.1002/app.41796**

LOW-FOULING POLYMERS

Low fouling polysulfone ultrafiltration membrane via click chemistry
Y. Xie, R. Tayouo and S. P. Nunes, *J. Appl. Polym. Sci.* 2015, **DOI: 10.1002/app.41549**

Elucidating membrane surface properties for preventing fouling of bioreactor membranes by surfactin
N. Behary, D. Lecouturier, A. Perwuelz and P. Dhulster, *J. Appl. Polym. Sci.* 2015, **DOI: 10.1002/app.41622**

PVC and PES-*g*-PEGMA blend membranes with improved ultrafiltration performance and fouling resistance
S. Jiang, J. Wang, J. Wu and Y. Chen, *J. Appl. Polym. Sci.* 2015, **DOI: 10.1002/app.41726**

Improved antifouling properties of TiO_2/PVDF nanocomposite membranes in UV coupled ultrafiltration
M. T. Moghadam, G. Lesage, T. Mohammadi, J.-P. Mericq, J. Mendret, M. Heran, C. Faur, S. Brosillon, M. Hemmati and F. Naeimpoor, *J. Appl. Polym. Sci.* 2015, **DOI: 10.1002/app.41731**

Development of functionalized doped carbon nanotube/polysulfone nanofiltration membranes for fouling control
P. Xie, Y. Li and J. Qiu, *J. Appl. Polym. Sci.* 2015, **DOI: 10.1002/app.41835**

JOURNAL OF Applied Polymer SCIENCE

Special Issue: Microfiltration and Ultrafiltration Membrane Science and Technology

Guest Editors: Prof. Isabel C. Escobar (University of Toledo) and
Prof. Bart Van der Bruggen (University of Leuven)

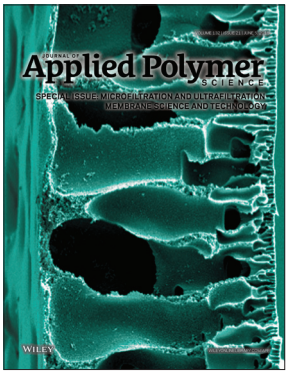

SURFACE MODIFICATION OF POLYMER MEMBRANES

Highly chlorine and oily fouling tolerant membrane surface modifications by *in situ* polymerization of dopamine and poly(ethylene glycol) diacrylate for water treatment
K. Yokwana, N. Gumbi, F. Adams, S. Mhlanga, E. Nxumalo and B. Mamba, *J. Appl. Polym. Sci.* 2015, **DOI: 10.1002/app.41661**

Fouling control through the hydrophilic surface modification of poly(vinylidene fluoride) membranes
H. Jang, D.-H. Song, I.-C. Kim, and Y.-N. Kwon, *J. Appl. Polym. Sci.* 2015, **DOI: 10.1002/app.41712**

Hydroxyl functionalized PVDF-TiO_2 ultrafiltration membrane and its antifouling properties
Y. H. Teow, A. A. Latif, J. K. Lim, H. P. Ngang, L. Y. Susan and B. S. Ooi, *J. Appl. Polym. Sci.* 2015, **DOI: 10.1002/app.41844**

Enhancing the antifouling properties of polysulfone ultrafiltration membranes by the grafting of poly(ethylene glycol) derivatives via surface amidation reactions
H. Yu, Y. Cao, G. Kang, Z. Liu, W. Kuang, J. Liu and M. Zhou, *J. Appl. Polym. Sci.* 2015, **DOI: 10.1002/app.41870**

SEPARATION APPLICATIONS

Experiment and simulation of the simultaneous removal of organic and inorganic contaminants by micellar enhanced ultrafiltration with mixed micelles
A. D. Vibhandik, S. Pawar and K. V. Marathe, *J. Appl. Polym. Sci.* 2015, **DOI: 10.1002/app.41435**

Polymeric membrane modification using SPEEK and bentonite for ultrafiltration of dairy wastewater
A. Pagidi, Y. Lukka Thuyavan, G. Arthanareeswaran, A. F. Ismail, J. Jaafar and D. Paul, *J. Appl. Polym. Sci.* 2015, **DOI: 10.1002/app.41651**

Forensic analysis of degraded polypropylene hollow fibers utilized in microfiltration
X. Lu, P. Shah, S. Maruf, S. Ortiz, T. Hoffard and J. Pellegrino, *J. Appl. Polym. Sci.* 2015, **DOI: 10.1002/app.41553**

A surface-renewal model for constant flux cross-flow microfiltration
S. Jiang and S. G. Chatterjee, *J. Appl. Polym. Sci.* 2015, **DOI: 10.1002/app.41778**

Ultrafiltration of aquatic humic substances through magnetically responsive polysulfone membranes
N. A. Azmi, Q. H. Ng and S. C. Low, *J. Appl. Polym. Sci.* 2015, **DOI: 10.1002/app.41874**

BIOSEPARATIONS APPLICATIONS

Analysis of the effects of electrostatic interactions on protein transport through zwitterionic ultrafiltration membranes using protein charge ladders
M. Hadidi and A. L. Zydney, *J. Appl. Polym. Sci.* 2015, **DOI: 10.1002/app.41540**

Modification of microfiltration membranes by hydrogel impregnation for pDNA purification
P. H. Castilho, T. R. Correia, M. T. Pessoa de Amorim, I. C. Escobar, J. A. Queiroz, I. J. Correia and A. M. Morão, *J. Appl. Polym. Sci.* 2015, **DOI: 10.1002/app.41610**

Hemodialysis membrane surface chemistry as a barrier to lipopolysaccharide transfer
B. Madsen, D. W. Britt, C.-H. Ho, M. Henrie, C. Ford, E. Stroup, B. Maltby, D. Olmstead and M. Andersen, *J. Appl. Polym. Sci.* 2015, **DOI: 10.1002/app.41550**

Membrane adsorbers comprising grafted glycopolymers for targeted lectin binding
H. C. S. Chenette and S. M. Husson, *J. Appl. Polym. Sci.* 2015, **DOI: 10.1002/app.41437**

Journal of Applied Polymer Science

Preparation and characterization of MOF-PES ultrafiltration membranes

Arcadio Sotto,[1] Gisela Orcajo,[1] Jesús María Arsuaga,[1] Guillermo Calleja,[1] Junkal Landaburu-Aguirre[2]

[1]Department of Chemical and Environmental Technology, Rey Juan Carlos University, Madrid, Spain

[2]Mass and Heat Transfer Process Laboratory, Department of Process and Environmental Engineering, P.O. Box 4300, FI-90014, University of Oulu, Finland

Correspondence to: A. Sotto (E-mail: arcadio.sotto@urjc.es)

ABSTRACT: Fouling is one of the main disadvantages of membrane processes. Fouling can be mitigated by incorporating inorganic particles into the membrane. Composite membranes containing the inorganic fillers show higher pore size, porosity, and hydrophilic character than the neat PES membrane, which contributes to a better permeability. In this research, PES ultrafiltration membranes are prepared using both commercial and synthesized metal-organic framework materials (MOF) as well as ZnO particles as fillers. Among the different fillers used, MOF particles produce a better effect on the permeability of the membrane than ZnO particles. The synthesized Zn/Co-MOF-74-type materials have good structural stability in the polymeric matrix and the MOF-PES membrane maintains its performance after a series of cycles of BSA water solution. Tested MOF-PES membrane also shows higher BSA rejections and permeate flux than the neat PES membrane, demonstrating that it is possible to enhance the flux without losing the selectivity of the membrane. © 2014 Wiley Periodicals, Inc. J. Appl. Polym. Sci. **2015**, *132*, 41633.

KEYWORDS: polycarbonates; porous materials; properties and characterization; surfaces and interfaces

Received 24 July 2014; accepted 14 October 2014

DOI: 10.1002/app.41633

INTRODUCTION

Membrane fouling is one the main disadvantages of the pressure-driven membrane processes applied to wastewater treatment.[1] Membrane fouling can be caused by mineral precipitation,[2] attachment of colloids and dissolved organics[3,4] and growth of microbes on the membrane surface.[5] As a consequence, permeate flux is reduced and salt passage through the membrane increases, decreasing the overall membrane process performance. As a consequence the membrane efficiency is reduced, being the water recovery level below the optimum. In addition, both the energy demand and the overall operational cost of the process increase.[6] These fouling mechanisms can be reversible or irreversible. Reversible fouling is caused by the formation of a cake layer (deposition) or concentration polarization (gel formation) of materials at the membrane surface. They can be removed by an appropriate physical washing such as backwashing or surface washing. Irreversible fouling, however, is caused by permanent adsorption and/or pore blockage by species present in the liquid. In order to improve the fouling tendency of membranes, research studies have focused on the introduction of hydrophilic layers, the reduction of surface roughness and the improvement of surface charge.[7] Another important development in antifouling pressure-driven membranes is the incorporation of nanoscale inorganic particles into the membrane. The use of nanoparticles in the synthesis of membranes can improve their performance by decreasing the degree of membrane fouling, and therefore increasing the permeate flux.[8,9] The hydrophobicity of both organic pollutants and the membrane surface (polymeric material) favors the presence of hydrophobic interactions in the surface-pollutant interface, which promotes the formation of a fouling layer onto the membrane surface and in the inner pore walls of the membrane structure.[10] The addition of hydrophilic fillers into the membrane composition mitigates the formation and progress of fouling phenomena taking into account the hydrophilic character of nanomaterials proposed as dopants.[11] Among these nanomaterials, TiO_2, SiO_2, ZrO_2, Al_2O_3, and Ag were found to improve anti-fouling performance of membranes. The increased hydrophilic character of the membranes containing Al_2O_3, reduces the chance of absorbing hydrophobic matter,[12] thus preventing colloidal and organic fouling. Membranes combined with silver benefit from the bactericidal activity of silver nanoparticles. Silver composite thin films have a less compact structure and a rougher surface than the pure polyamide films. These membranes were shown to have a great anti-biofouling performance, but the release of silver is likely to influence the long-lasting antibacterial and biofouling resistant performance.[13]

The environmental risk associated to the use of nanomaterials and the integrity of membrane functions are additional issues associated to the use of nanoparticles in aqueous environments.[14]

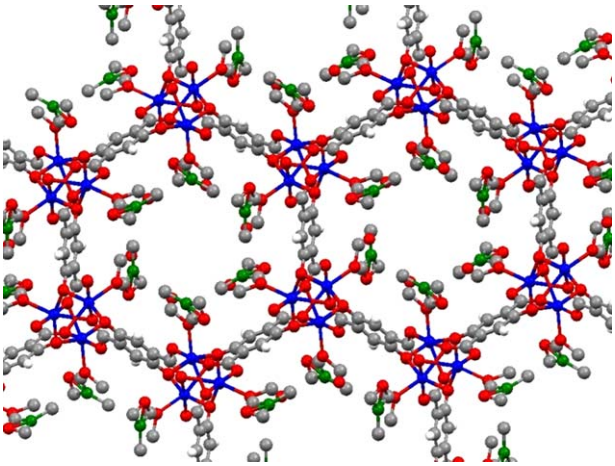

Figure 1. Two-dimensional view of the honeycomb-like $Me_2(dhtp)$ (CH_3OH) structure. [Color figure can be viewed in the online issue, which is available at wileyonlinelibrary.com.]

It has been previously demonstrated that the weight percent of nanoparticles is reduced after the permeation tests.[15] This indicates that the nanoparticles would leach out during the test because of the weak interaction with the membrane matrix. In addition, it has been previously reported that nano-ZnO has low water stability being decomposed to toxic Zn^{2+},[16,17] which creates a risk for the ecosystem. This may limit the applicability of nano-ZnO particles in membrane processes.

Membrane stability could be improved by increasing the interface compatibility between nano-fillers and the polymeric matrix. For this purpose, a new class of materials consisting of inorganic moieties linked together by organic bridges, called Metal-Organic Framework (MOF), can be good alternatives compared to the commonly used metal oxides, so that using MOF materials in ultrafiltration membranes seem to be a promising area of research. MOF materials show intrinsic properties that could favor the membrane performance: (1) they are constituted by metal or metal clusters bounded to multifunctionalized organic molecules such as amines, pyridines, carboxylates, sulphonates, and phosphonates, providing a wide variety of crystalline porous materials, (2) they can have different porous structures that can act as molecular sieves, and (3) they have extraordinary surface area and free pore volume. In other words, by selecting the suitable components, a especific MOF structure with the desired physico-chemical properties can be designed.[18] Concerning MOF stability, Küsgens *et al.*[19] studied the water adsorption of MOFs, showing that commercial ZIF-8 has a remarkable chemical stability towards water, maintaining the MOF framework structure after a heating treatment in water

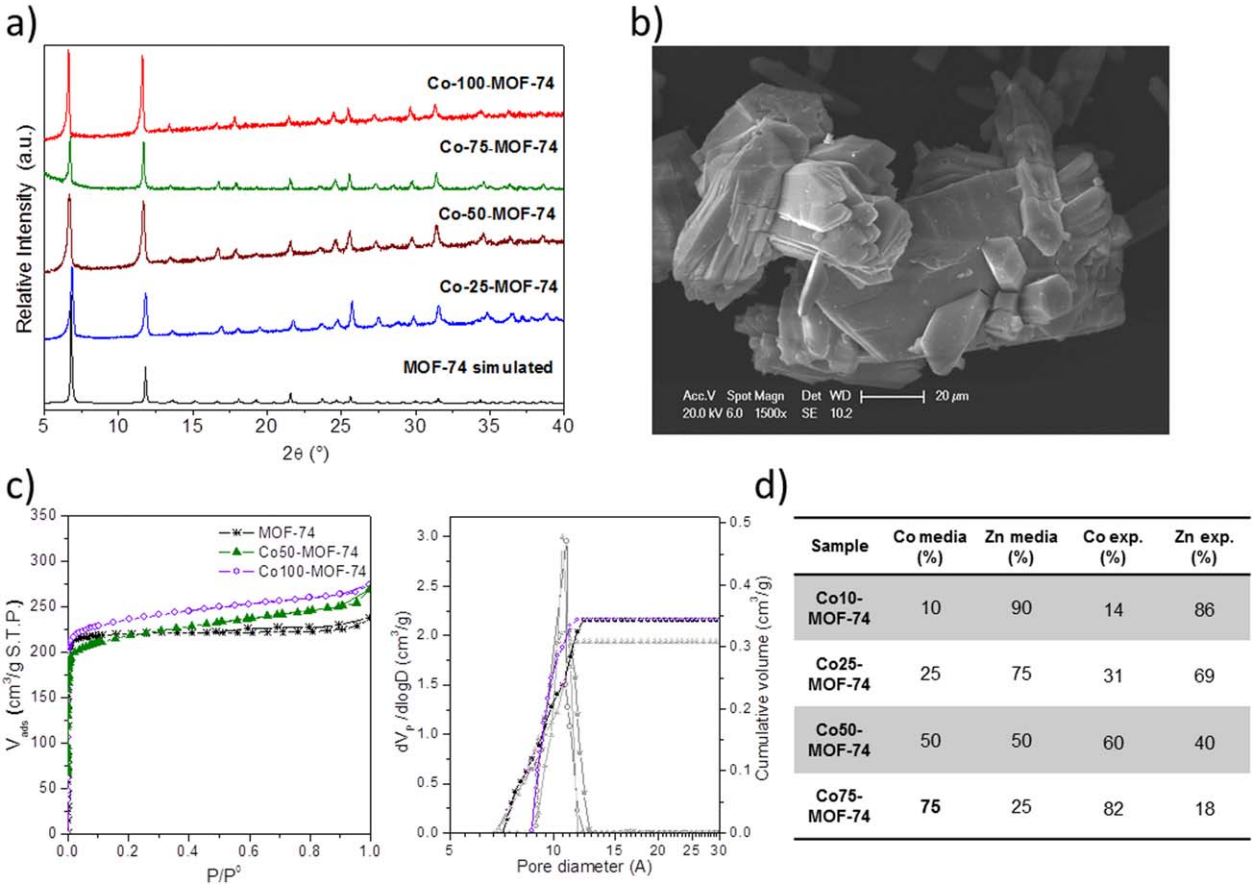

Sample	Co media (%)	Zn media (%)	Co exp. (%)	Zn exp. (%)
Co10-MOF-74	10	90	14	86
Co25-MOF-74	25	75	31	69
Co50-MOF-74	50	50	60	40
Co75-MOF-74	75	25	82	18

Figure 2. Zn/Co-MOF-74 materials employed for membrane synthesis: (a) XRD patterns, (b) SEM image, (c) Nitrogen adsorption-desorption isotherm and pore size distribution, and (d) Co incorporation in MOF-74 material. [Color figure can be viewed in the online issue, which is available at wileyonlinelibrary.com.]

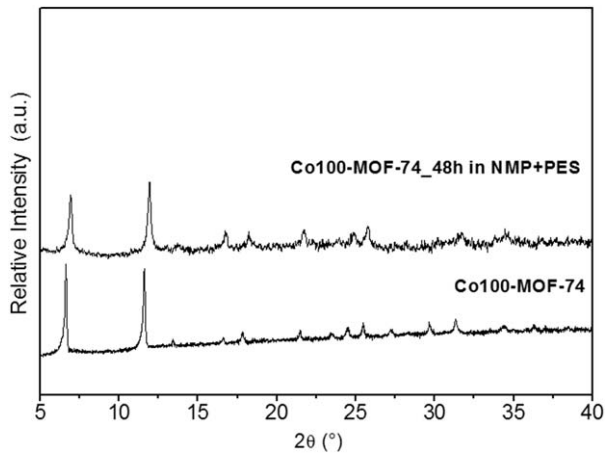

Figure 3. XRD patterns of Co100-MOF-74 before and after being submerged in PES/NMP solution.

for 24 h at 323 K. This stability reinforces the potential application of polymer-MOF mixture matrix membranes for water purification.

During the last decade several groups have focused their efforts on the preparation of three-dimensional honeycomb-like metal–organic frameworks using 2,5-dihydroxyterephthalic acid (H_2dhtp) as an organic linker (Figure 1). The use of this linker in the presence of different divalent metal ions such as Zn^{2+}, Mg^{2+}, Ni^{2+}, Fe^{2+}, Co^{2+} has resulted in the MOF-74 structure,[20–25] with exposed and unsaturated metal sites, which are available for interacting with any particular substrate. Mixed-metal MOF-74 structures that contain simultaneously Zn^{2+} and Co^{2+} metal ions have been developed by our group,[26] demonstrating that the coexistence of both transition metal ions in the MOF-74 framework enhances the interaction with some particular adsorbate molecules.

In this article, the addition of tailor made Zn/Co- MOF -74 particles and commercial ZIF-8 metal organic framework particles to ultrafiltration membrane is studied. The main goal is to evaluate the effect of MOF fillers on the membrane morphology and performance, as well as to compare the behavior of synthesized Zn/Co-MOF-74 particles and ZIF-8 particles as well as the commonly used ZnO particles.

EXPERIMENTAL

Synthesis and Characterization of MOF Nanocrystals

Zn- and Co- containing MOF-74 materials were prepared following the procedure published elsewhere,[26] in which 2,5-dihydroxybenzene-1,4-dicarboxylic acid (H_2dhtp, from Sigma-Aldrich S.L.), tetrahydrated zinc nitrate and/or hexahydrated cobalt nitrate (Fluka) were added over N,N-dimethylformamide (DMF, from Scharlab S.L.) under stirring. Once these reagents were dissolved, de-ionized water was added to form a clear solution of molar composition: 1H_2DHBDC: 2.9 (Zn-Co) : 523 DMF : 107H_2O. This mixture was heated up to 100°C for 20 h to yield needle shaped crystals. After decanting the hot mother liquor and washing with DMF, the solid product was immersed in methanol for 6 days. During this period of time the solvent was renewed three times after solid decanting. Methanol was finally removed under high vacuum ($<10^{-7}$ bar) at 150°C, yielding a porous material with MOF-74 structure.

MOF phase identification was carried out by X-ray powder diffraction (XRD) using a PHILIPS X'PERT diffractometer with Cu Kα radiation. Nitrogen adsorption–desorption isotherms at −196°C were measured using an AutoSorb equipment (Quantachrome Instruments). The pore surface area was calculated by using the Brunauer–Emmett–Teller (BET) model. The pore volume and diameter were estimated by non-local DFT calculations.

The metal oxide and MOF particle size distributions were determined by using digital imaging and analysis processing from the Scanning Electron Microscopy images (SEM, XL-30, Philips, Eindhoven, the Netherlands).

Preparation and Characterization of MOF-PES Ultrafiltration Membranes

Polyethersulfone (PES) supplied by BASF (Germany) was employed as the base polymer. 1-Methyl-2-pyrrolidone (NMP, 99.5%) provided by Sharlab (Spain) was used as the polymer solvent. The support layer (Viledon FO2471) used for the PES membrane manufacturing was obtained from Freudenberg (Weinheim, Germany).

Neat and doped membranes were prepared using phase inversion induced by immersion precipitation technique. PES polymer (at 20 wt %) was dissolved in NMP. Doped membranes were prepared by dispersing 0.4 g of filler particles in 79.6 mL of solvent for 3 h by mechanical stirring at 200 rpm and room temperature. Subsequently, 20 g of polymer to the particle/solvent solution was added and stirred for 24 h at 500 rpm and 40°C. After formation of an homogenous solution, the films were cast with 200 μm thickness with a filmograph on nonwoven polyester as a support layer. The membrane films were immersed in the non-solvent bath (distilled water at 20°C) for precipitation. The membrane was afterwards repeatedly washed with distilled water to remove the remaining solvent. For each polymer solution composition, five identical membrane sheets were made and tested to obtain an average value of flux and solute rejection.

The hydrophilicity of membrane skin surface was determined on the basis of a water contact angle system (DSA 10 Mk2 Krüss, Germany) equipped with video capture at room temperature. A water droplet was placed on a dry, flat and homogeneous membrane surface and the contact angle between water and membrane was measured was observed. The average contact angle for distilled water was determined for six measurements on the different membrane surfaces.

The morphologies of membranes cross-section were observed by SEM. The membranes were cut in pieces of small sizes and frozen with liquid nitrogen, to produce a crio-fracture on the cross section. The samples were dried and kept in vacuum conditions, and then were gold sputtered (13–15 nm thickness). The surface pore size distribution of the membranes was characterized by Field Emission Gun Scanning Electron Microscope (FEGSEM, FEI, the Netherlands). Membrane specimens were sputtered with platinum (5 nm thickness).

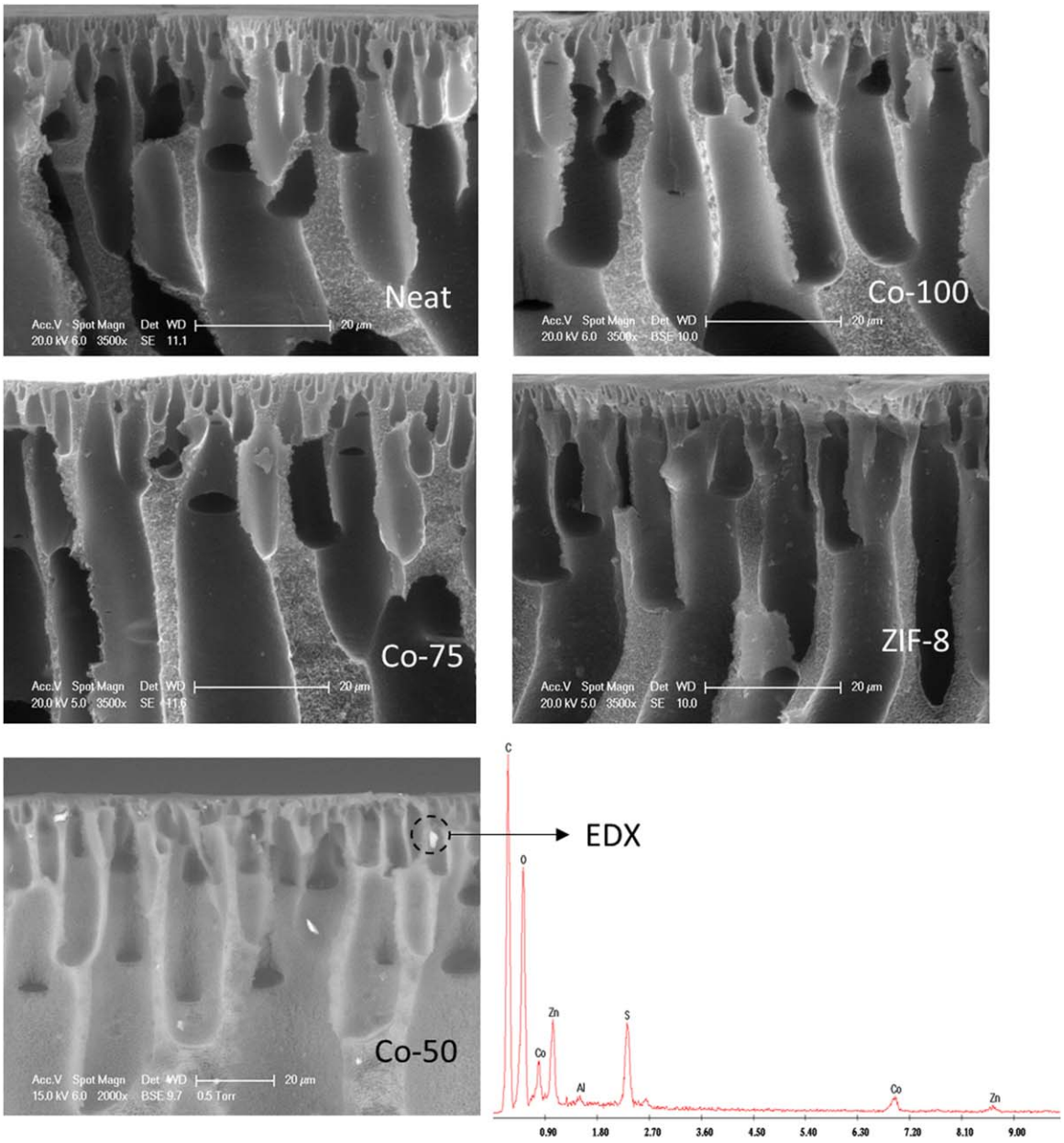

Figure 4. SEM images of membranes cross-section. [Color figure can be viewed in the online issue, which is available at wileyonlinelibrary.com.]

The overall membrane porosity (P_r,%) was calculated as a function of the membrane weight using the following equation:

$$P_r(\%) = \left(\frac{W_w - W_d}{Sd\rho}\right) \times 100 \quad (1)$$

where W_w and W_d are the membrane weight of at equilibrium in swollen and dry state, respectively; S the membrane area; d the membrane thickness and ρ the water density. The membranes were immersed in water during 24 h prior to measurement of swelling state. The porosity data were the average of four measurements with four samples of each membrane.

Ultrafiltration Experiments

The prepared membranes were characterized for water flux using a cross-flow filtration set-up.[27] A constant feed composition was achieved by recycling the retentate and permeate stream to the feed tank. In a typical run, membranes were compacted using Milli-Q water for 2 h at 3 bar until there was no further variation in permeate flux, then the water flux was recorded. In this way the influence of compaction during filtration experiments could be avoided. After compaction, the pure water permeability was determined by measuring the pure water flux during 2 h at 25°C.

In order to study the effect of membrane fouling, the membranes were tested in a cross-flow filtration equipment in recycle mode fed with 200 mg/L of BSA. The permeate flux and rejection of all membranes were determined at 2 bar transmembrane pressure at 25°C. Concentration polarization was minimized by using a cross-flow velocity of 4.5 m/s. This feed

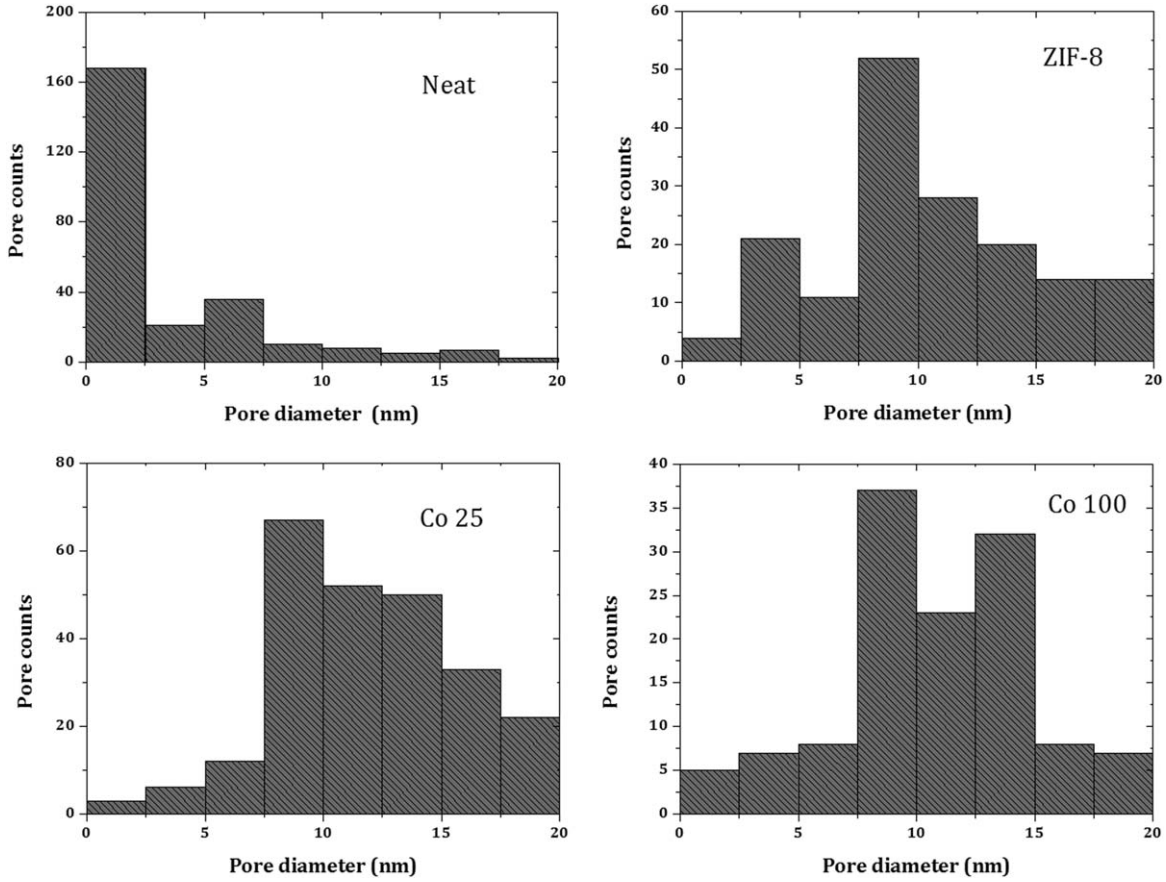

Figure 5. Pore size distribution of neat and some doped membranes.

velocity corresponds to a Reynolds number of 30,000, which is far in the turbulent region.

RESULTS AND DISCUSSION

Synthesis and Characterization of MOF Nanocrystals

The most relevant characterization data of synthesized Zn/Co-MOF-74 materials is depicted in Figure 2. For all materials with different Zn/Co ratios [Figure 2(a)], powder X-ray diffraction patterns showed the typical reflections of MOF-74 phase,[20] characteristic of the three-dimensional coordination structure with a honeycomb topology that contains 1-D broad channels (Figure 1). SEM micrograph [Figure 2(b)] revealed the expected large needle-shaped crystals for all materials synthesized, similar to those previously published.[26] The porosity of the MOF-74-type materials was measured by nitrogen adsorption/desorption at −196°C [Figure 2(c)]. The type I isotherms revealed a permanent microporosity with a BET specific surface area around 1000 m^2/g, a pore volume of 0.5 cm^3/g and an average pore diameter of ca. 11 Å. The thermogravimetric analysis in N_2 atmosphere (not shown) indicates the decomposition of the organic moiety of the sample above 250°C for all obtained materials. This fact is a clear evidence of the thermal stability of the MOF-74 framework at high temperatures.

Before preparing the MOF-PES membranes, the stability of MOF-74 structure in the synthesis media of the polymeric membrane was studied, by submerging the Co100-MOF-74 material in a PES/NMP solution during 48 h at room temperature. As it can be observed in the XRD patterns (Figure 3), the treated material shows structural stability of the MOF framework under the membrane synthesis conditions. A direct XRD analysis of the MOF-matrix membrane would be useless since the amount of MOF in the membrane is very low, being under the detection limit of this technique.

Morphological Characterization of MOF-PES Ultrafiltration Membranes

The morphology of manufactured membranes was explored by SEM technique, observing the cross-section of membranes (Figure 4).

As shown, the membranes show a typical macrovoid-like structure in its morphology due to the formation of polymer-lean phase zones into the polymeric solution configuration during the phase inversion process.[28] The main relevant differences observed in the morphology of doped membranes compared to the neat PES membrane are a decrease of skin membrane layer thickness and an enhanced connectivity and uniformity of pores along the membrane structure. As a consequence of these morphological changes, it is expected to observe an increase of water transport through the membrane, i.e., a higher membrane permeability.

The membrane morphology was also explored in terms of surface membrane porosity as shown in Figure 5.

The addition of MOF fillers resulted in an increase of average pore size of doped membranes. The presence of doping particles

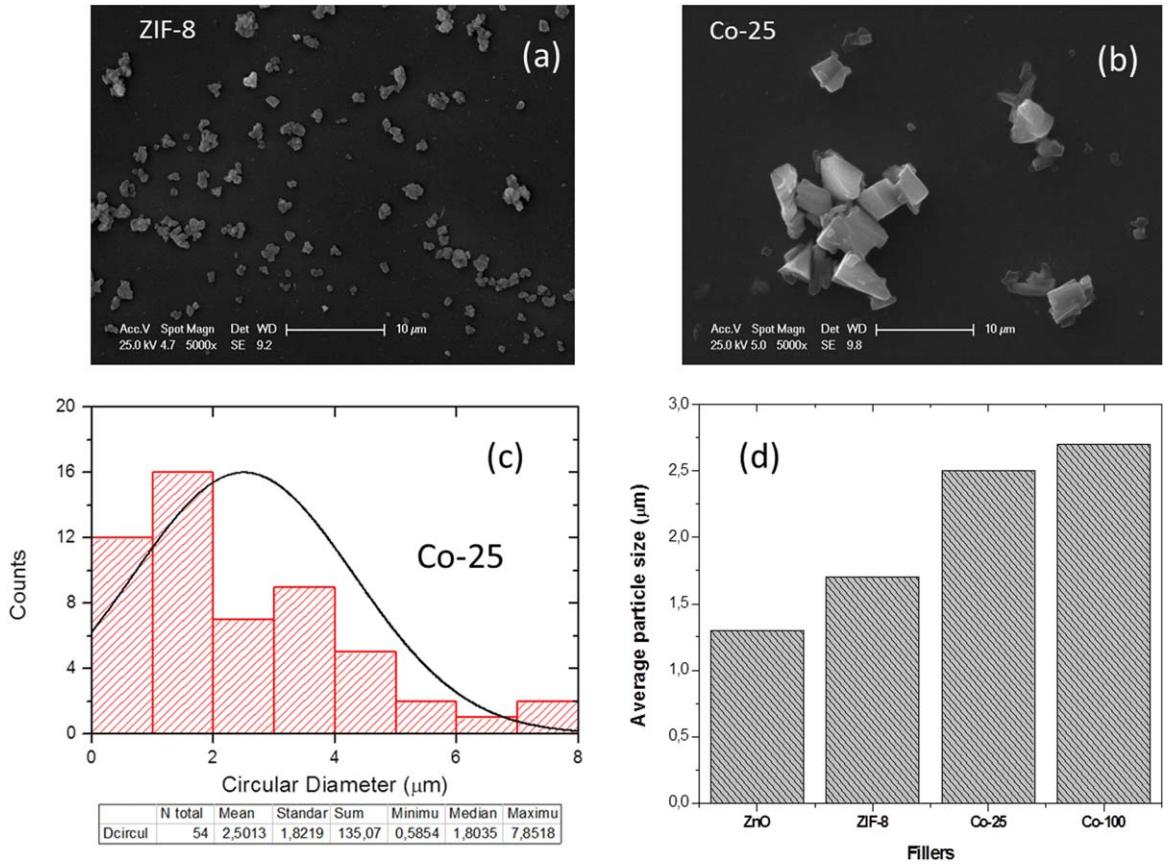

Figure 6. Average particle size of some used fillers. [Color figure can be viewed in the online issue, which is available at wileyonlinelibrary.com.]

in the polymeric solution increases the number of lean-polymer phase zones, promoting the pore formation onto the membrane surface. This effect has been revealed by other authors considering the fillers as pore forming agents.[11,29] In addition, the membranes doped with MOF-74 material exhibited larger pore sizes than the membranes doped with ZIF-8. Taking into account that the presence of particles disturbs the interaction of polymer chains during the membrane formation, the size of filler particles incorporated into the polymer matrix could determine the extent of lean-polymer phase zones Considering the average particle size of MOFs displayed in Figure 6, the formation of bigger areas could be expected, with lower polymer chain density, which results in membranes with high pore sizes. The effect of particle size on the membrane morphology has been clarified in a previous work.[12]

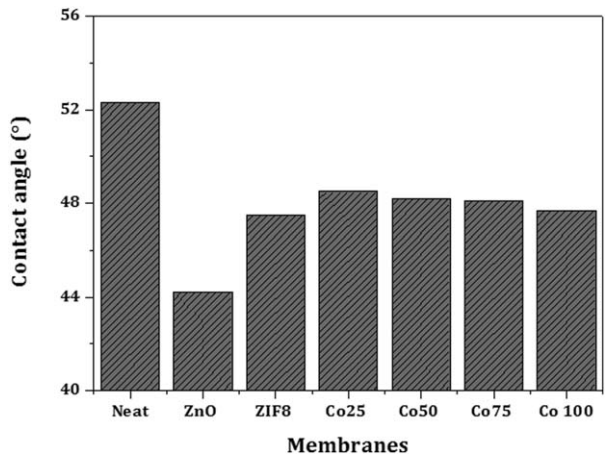

Figure 7. Contact angle of the neat and mix matrix membranes prepared.

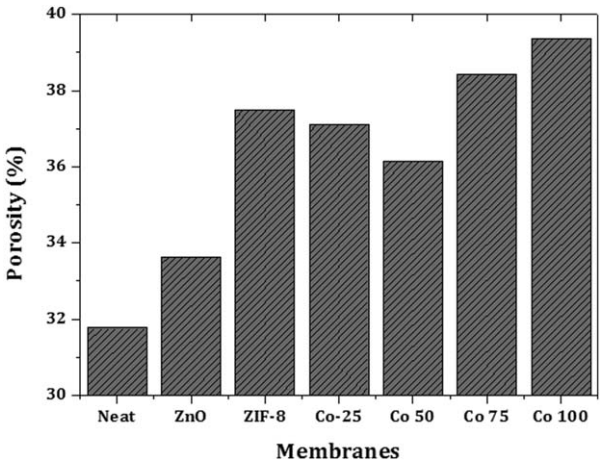

Figure 8. Porosity of neat and doped membranes.

The surface hydrophilicity of membranes was explored by contact angle experiments (Figure 7). Assuming constant polymer

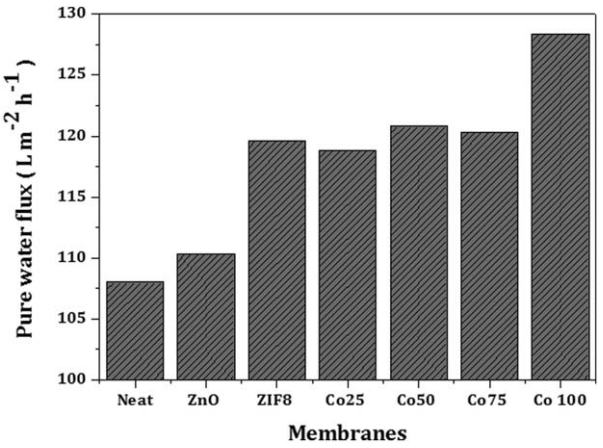

Figure 9. Membranes permeability determined at 2 bar of transmembrane pressure.

and filler concentrations during preparation of doped membranes, the observed differences of the contact angles should be attributed to the effect of the fillers on the casting solution. The neat PES membrane exhibited the most hydrophobic surface. The incorporation of hydrophilic fillers near the membrane skin layer decreased the contact angles of water droplets deposited onto the membrane surface. This effect could be explained by the higher affinity of metal oxide and metal clusters of MOFs to water, strengthening the interaction between them and hence the membrane surface wetting. In addition, when pore diameter increases (Figure 5), more water can be absorbed by the membrane structure during the contact angle experiments. The lowest contact angle observed for the ZnO doped membrane can be associated to the highest metal content of this filler type in comparison with the absolute metal content in MOFs particles.

The membrane porosity was also investigated by water-uptake experiments as shown in Figure 8. In general, the incorporation of particles promoted an increase of free volume into the membrane structure. In comparison with metal oxide (ZnO) the addition of MOFs into the membrane structure showed a more pronounced effect on the membrane porosity. It is difficult to relate these results with the macrovoid configuration of the polymer matrix observed for the tested membranes (Figure 4); however, the presence of less dense top layer and better connectivity between the surface and inner pores of MOFs doped membrane could increase the water absorption by the membrane.

Membrane Permeation

Ultrafiltration experiments were carried out to study the permeation performance of the synthesized membranes. Pure water membrane flux was measured when the membrane performance reached the stationary state on flux Figure 9 shows the membrane permeation potential in terms of pure water flux.

The addition of particles to membranes enhances the water flux through them, due to the increased hydrophilic character of the PES membranes when adding the fillers. As previously explained, the higher affinity of metal oxide and metal clusters of MOFs for water increases the hydrophilicity of the membrane and consequently the pure permeate flux also increases. Comparing the pure water flux among the membranes with MOF materials, it can be observed that the membrane containing Co-100-MOF 74 material shows the highest water permeate flux, possibly due tothe higher porosity of the membrane. As observed in Figure 8, the membrane with Co-100-MOF 74 shows the largest porosity leading to a higher permeability.

In order to explore the selectivity and fouling performance of the membranes, permeation experiments for 200 mg/L BSA solution were conducted at 2 bar of transmembrane pressure as shown in Figure 10.

In all cases the doped membranes exhibited higher fluxes than the neat PES membrane, increasing the rejection as result of MOF particle incorporation. This last effect is very interesting considering the desired balance between permeation and selectivity of membranes. Considering the steric interaction between the membrane and the solute, it is common to observe a reverse trend between permeation and rejection as a result of increased membrane average pore size. In this study, adsorption of BSA molecules onto the surface and inner structure of membranes is prevented by the hydrophilic character of doping particles, leading to higher values of flux and rejection. The undesired hydrophobic interactions that take place between the model foulant (BSA) and the polymeric material are mitigated by the

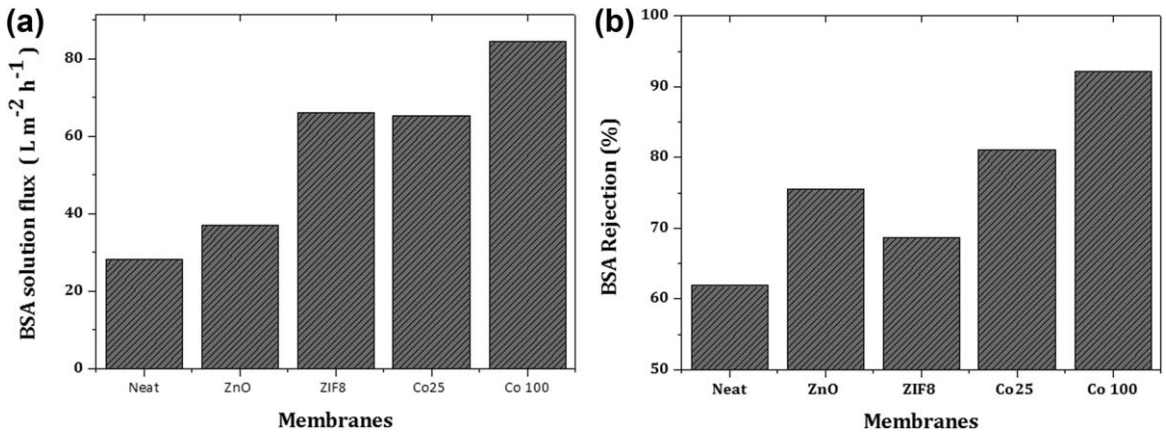

Figure 10. (a) Permeate flux and (b) rejections for BSA aqueous solution obtained using prepared membranes.

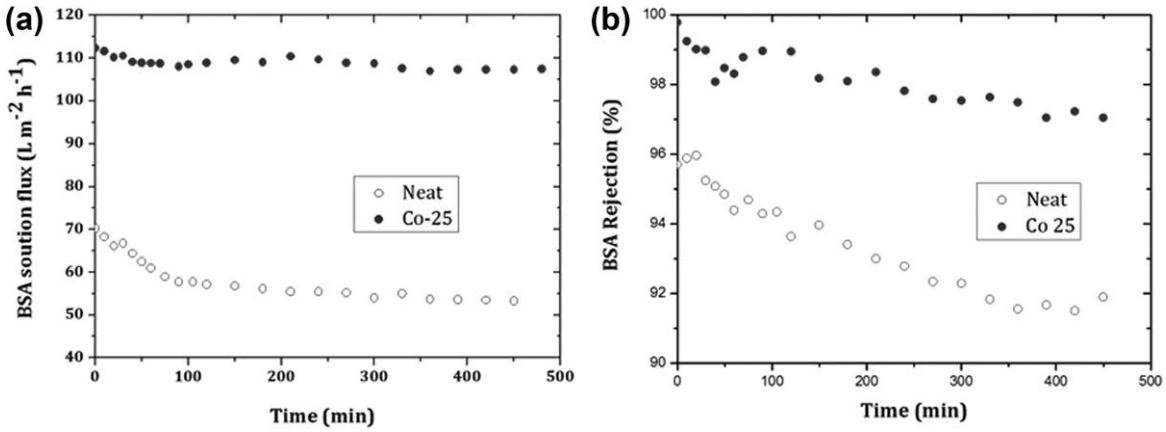

Figure 11. Permeate flux and rejections of neat and Co 25-MOF-74 PES membranes for BSA aqueous solutions.

incorporation of hydrophilic particles leading to an enhanced membrane performance. In order to support this hypothesis, a comparison of membrane flux and BSA rejection for neat and Co25 doped membranes was accomplished, as shown in Figure 11.

The accumulation of foulants onto the membrane pore acts as a driving force for the diffusion of hydrophobic molecules through the membrane structure, affecting negatively to both the water permeation and the rejection potential of membranes. At the beginning of the filtration experiment (during the first 100 min) the neat membrane flux declined, decreasing at the same time the BSA rejection by the membrane. However, the doped membrane exhibited a stationary state in its permeation that hardly affected the selectivity of Co 25 membrane.

Finally, membrane stability was evaluated by measuring the permeate flux of the membrane containing Co-100-MOF 74 material in four different cycles of BSA solution filtration. Between each cycle the membrane was cleaned with distilled water for 1 h. As observed in Figure 12, the permeate flux decreased slightly after the first cycle. However, in the rest of the cycles the permeate flux was maintained in the same flux values showing the good stability of the membrane.

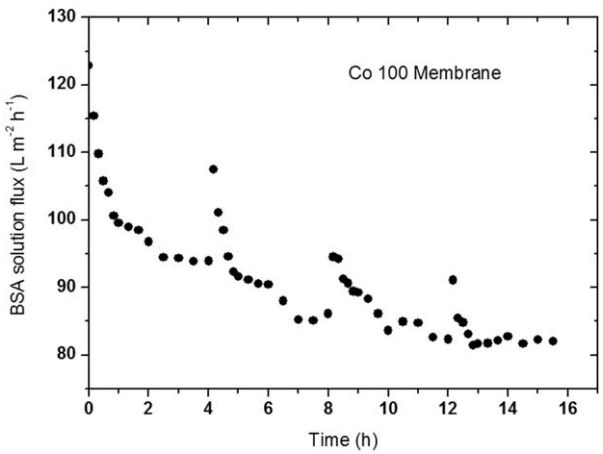

Figure 12. Permeate flux of four different cycles of BSA solution filtration using the PES membrane containing Co-100-MOF-74 material.

CONCLUSIONS

In this study PES ultrafiltration membranes were prepared using different metal organic framework materials and ZnO particles as fillers. The addition of the fillers into the membrane affected the morphology of the PES membrane, resulting in membranes with thinner skin and improved connectivity between the macrovoids. In addition, by adding the fillers, the porosity, the pore size and the hydrophilic character of the membrane increased, enhancing the permeability of the membrane. Among the different fillers used, the MOF particles affected more significantly the permeability of the membrane than ZnO particles.

BSA rejections obtained using the Co-25-MOF-74 membrane were higher than the rejections of the neat PES membrane. These results are very significant since they show that successful rejection coefficients can be obtained without sacrificing the permeate flux of the membrane.

Overall, this study has shown that MOF materials are potential materials to be incorporated in the preparation of membranes. The synthesized Zn/Co-MOF-74 materials showed good structural stability in the polymeric membrane, proving the applicability of these materials as fillers in membrane preparation processes. Moreover, it was shown that MOF-74-type and ZIF-8 particles enhance more the membrane performance than ZnO particles, becoming clear alternatives to the commonly used metal oxide nano-fillers. Further, PES-MOF matrix membranes showed to be stable over various cycles of BSA solution filtration, demonstrating the potential applicability of these mix matrix membranes for water purification purposes.

REFERENCES

1. Verliefde, A.; Sotto, A.; Kim, J.; Van der Bruggen, B. In Nanotechnology for Water Purification; Day, T.; Ed.; Brown Walker Press: Boca Raton, Florida, **2012**; Chapter 8, p 179–209.

2. Waly, T.; Kennedy, M. D.; Witkamp, G. T.-J.; Amy, G.; Schippers, J. C. *Desalination* **2012**, *284*, 279.
3. Tang, C. Y.; Chong, T. H.; Fane, A. G. *Adv. Colloid Interface Sci.* **2011**, *164*, 126.
4. Lee, S.; Choi, J.-S.; Lee, C.-H. *Desalination* **2009**, *238*, 109.
5. Kim, D.; Jung, S.; Sohn, J.; Kim, H.; Lee, S. *Desalination* **2009**, *238*, 43.
6. Nguyen, T.-V.; Pendergast, M. T. M.; Phong, M. T.; Jin, X.; Peng, F.; Lind, M. L.; Hoek, E. M. V. *Desalination* **2014**, *338*, 1.
7. Tang, C. Y.; Chong, T. H.; Fane, A. G. *Adv. Colloid Interface Sci.* **2011**, *164*, 126.
8. Sotto, A.; Boromand, A.; Zhang, R.; Luis, P.; Arsuaga, J. M.; Kim, J.; Van der Bruggen, B. *J. Colloid Interface Sci.* **2011**, *363*, 540.
9. Kim, S. H.; Kwak, S.-Y.; Sohn, B.-H.; Park, T. H. *J. Membr. Sci.* **2003**, *211*, 157.
10. Qu, F.; Liang, H.; Zhou, J.; Nan, J.; Shao, S.; Zhang, J.; Li, G. *J. Membr. Sci.* **2014**, *449*, 58.
11. Hoek, E. M. V.; Ghosh, A. K.; Huang, X.; Liong, M.; Zink, J. *Desalination* **2011**, *283*, 89.
12. Arsuaga, J. M.; Sotto, A.; del Rosario, G.; Martínez, A.; Molina, S.; Teli, S. B.; de Abajo, J. *J. Membr. Sci.* **2013**, *428*, 131.
13. Mollahosseini, A.; Rahimpour, A.; Jahamshahi, M.; Peyravi, M.; Khavarpour, M. *Desalination* **2012**, *306*, 41.
14. Crock, C. A.; Rogensues, A. R.; Shan, W.; Tarabara, V. V. *Water Res.* **2013**, *47*, 3984.
15. Taurozzi, J. S.; Arul, H.; Bosak, V. Z.; Burban, A. F.; Voice, T. C.; Bruening, M. L.; Tarabara, V. V. *J. Membr. Sci.* **2008**, *325*, 58.
16. Reed, R. B.; Ladner, D. A.; Higgins, C. P.; Westerhoff, P.; Ranville, J. F. *Environ. Toxicol. Chem.* **2012**, *31*, 93.
17. Li, Q. L.; Mahendra, V.; Lyon, D. Y.; Brunet, L.; Liga, M. V.; Li, D.; Alvarez, P. J. *J. Water Res.* **2008**, *42*, 4591.
18. Furukawa, H.; Cordova, K. E.; O'Keeffe, M.; Yaghi, O. M. *Science* **2013**, *341*, 974.
19. Küsgens, P.; Rose, M.; Senkovska, I.; Fröde, H.; Henschel, A.; Siegle, S.; Kaskel, S. *Microporous Mesoporous Mat.* **2009**, *120*, 325.
20. Rosi, N.; Kim, J.; Eddaoudi, M.; Chen, B.; O'Keeffe, M.; Yaghi, O. M. *J. Am. Chem. Soc.* **2005**, *127*, 1504.
21. Rowsell, J.; Yaghi, O. M. *J. Am. Chem. Soc.* **2006**, *128*, 1304.
22. Bhattacharjee, S.; Choi, J.-S.; Yang, S.-T.; Choi, S.; Kim, J.; Ahn, W.-S. *J. Nanosci. Nanotechnol.* **2010**, *10*, 135.
23. Dietzel, P.; Morita, Y.; Blom, R.; Fjellv, H. *Angew. Chem. Int. Ed.* **2005**, *44*, 6354.
24. Dietzel, P.; Panella, B.; Hirscher, M.; Blom, R.; Fjellv, H. *Chem. Commun.* **2006**, 959.
25. Dietzel, P. D. C.; Johnsen, R. E.; Blom, R.; Fjellvåg, H. *Chem. Eur. J.* **2008**, *14*, 2389.
26. Botas, J. A.; Calleja, G.; Sánchez-Sánchez, M.; Orcajo, G. *Int. J. Hydrogen Energy* **2011**, *36*, 10834.
27. Arsuaga, J. M.; Sotto, A.; López-Muñoz, M. J.; Braeken, L. *J. Membr. Sci.* **2011**, *372*, 380.
28. Boom, R. M.; Wlenk, I. M.; van den Boomgaard, Th.; Smolders, C. A. *J. Membr. Sci.* **1992**, *73*, 277.
29. Vatampour, V.; Esmaeili, M.; Farahani, M. H. D. A. *J. Membr. Sci.* **2014**, *466*, 70.